

## Direct oxidation of benzene to phenol in liquid phase by H<sub>2</sub>O<sub>2</sub> over vanadium catalyst supported on highly ordered nanoporous silica

J. Gholami<sup>a</sup>, A. R. Badiei<sup>a,\*</sup>, G. Mohammadi Ziarani<sup>b</sup>, A. R. Abbasi<sup>a</sup>

<sup>a</sup>School of Chemistry, College of Science, University of Tehran, Tehran, Iran

<sup>b</sup>Department of Chemistry, Faculty of Science, Alzahra University, Tehran, Iran

### Article history:

Received 28/10/2011

Accepted 23/12/2011

Published online 1/1/2012

### Keywords:

Benzene

Oxidation

Nanopore

Phenol

### \*Corresponding author:

E-mail address:

abadiei@khayam.ut.ac.ir

### Abstract

Vanadium supported on highly ordered nanoporous silica (VO<sub>x</sub>-LUS-1) was synthesized and characterized by XRD, Nitrogen adsorption desorption isotherms and UV-visible spectrophotometer. Direct oxidation of benzene to phenol in liquid phase by H<sub>2</sub>O<sub>2</sub> peroxide was examined by using various solvents (methanol, acetone, acetic acid, acetonitril). The maximum yield (25%) and selectivity (73%) of the phenol produced were obtained in the presence of acetic acid. The catalyst can be reused for several times without any appreciable loss of activity.

2012 JNS All rights reserved

## 1. Introduction

Phenol acts an important role as intermediate in the manufacture of petrochemicals, agrochemicals and plastics processes which is currently carried out through the Cumene process or toluene

oxidation. The global production of phenol (about 8 Mt/year) is mainly produced by the three-step Cumene process [1-2]. From economic point of view, this process depends strongly on the marketability of acetone (as a byproduct). The low yield and the energy consuming (three-steps) of

this process [3], has provoked the development of new routes to produce phenol free of byproduct. Recently, one step production of phenol with high yield and selectivity has grown enormously [3–8]. The first direct oxidation of benzene to phenol has been previously reported using Fenton reagent (ferrous sulfate-hydrogen peroxide) [9]. This oxidation reaction by using Hydrogen peroxide as an oxidant has been studied over titanium silicalite-1 (TS-1) in the solvent-free triphase conditions [7]. Corma et al. have designed Sn-beta zeolite and Sn-MCM-41 heterogeneous catalysts for the reaction of aromatic aldehydes with hydrogen peroxide in non halogenated solvents such as dimethylformamide and dioxane [8]. High selectivities of the corresponding phenol have been obtained by employing ethanol or aqueous acetonitrile as solvent with Sn-Beta. The liquid phase hydroxylation of benzene to phenol using hydrogen peroxide studied over Ti-, V-, Mg-, Fe-, Co-, and Cu-containing catalysts [10]. Only vanadium catalysts showed both high selectivity and sufficient activity [11-14].

Highly ordered nanoporous silica such as MCM-41 [1], LUS-1 [2-3], and SBA-15 [4] with very high surface area, uniform open form structure and extremely narrow pore size distribution has great potential for application in many fields such as catalysts. Recently, hydroxylation of benzene with hydrogen peroxide have been carried out using vanadium supported MCM-41 [15] SBA-15 [16]. However, relatively low yield for hydroxylation of benzene to give phenol was reported in literature. This motivated us to investigate the reaction by new support and reaction conditions to improve the yield and selectivity of phenol. In the present study, vanadium catalyst containing VOx species on high surface area supports of LUS-1 was synthesized and examined in benzene

hydroxylation with hydrogen peroxide, using a various solvents (methanol, acetone, acetic acid, acetonitrile). The purpose of this study is a significant improvement of catalytic performance. The maximum yield (25%) and selectivity (73%) of the phenol produced were obtained in the presence of acetic acid.

## 2. Experimental

### 2.1. Materials

Silica gel (60), Sodium hydroxide, n-decane, ammonium monovanadate, benzene, hydrogen peroxide (30%) and cetyltrimethylammoniumbromid (Merck) and P- toluenesulfonic acid monohydrate (Aldrich), of analytical grad were used without further purification.

### 2.2. Preparation of Catalysts

The preparation methods of the following nanoporous silica LUS-1 were described in our previous reports [17-18]. Deposition of  $\text{NH}_4\text{VO}_3$  complex on to the LUS-1 surface was carried out by the liquid-phase immobilizes method. About 3 g of uncalcined LUS-1 was stirred in 100 ml of  $\text{H}_2\text{O}$  solution containing 0.14 g of  $\text{NH}_4\text{VO}_3$  complexes for 3 h at room temperature. The solids were then filtered and washed with  $\text{H}_2\text{O}$  to remove the excess metal complexes. The filtered samples were dried under vacuum followed by heating at 120 °C for 2 h.

### 2.3. Spectrophotometric measurements

The electronic absorption spectra of solids were measured by adding the materials to spectral grade n-decane using a quartz window with about 0.5

mm path length. Very low light scattering was obtained from clear solid in n-decane. Since the reflective index of n-decane is very close to that of silica LUS-1, therefore good quality spectra were obtained.

#### 2.4. Catalytic tests in the liquid-phase hydroxylation

The catalytic activities were evaluated by the reaction of benzene and hydrogen peroxide 30% using various compounds as a solvent under reflux. A typical catalytic condition is the following: 0.1 g of catalyst was placed in a 50-mL round bottom flask with a condenser, and then 1ml of benzene in 11 mL of solvent solution was added. The mix was stirred for 5 min, then 2 ml of H<sub>2</sub>O<sub>2</sub> (30% in aqueous solution) were added. The reaction was carried out for 3 h at 60 °C under vigorous stirring. After the reaction was finished, the product mixture was cooled down to room temperature. The catalyst particle was filtered and then the reaction product was analyzed by a GC.

#### 2.5. Characterization techniques

Vanadium contents of the samples were analyzed with simultaneous inductively coupled plasma (ICP) allied analytical system (Jarrel-Ash, Model ICAP 9000). UV-visible spectra were taken on a Ray Leigh UV-1600 spectrophotometer. Nitrogen adsorption and desorption isotherms were measured at -196 °C using a Belsorp II system after the samples were vacuum dried at 150 °C

overnight. Powder X-ray diffractograms was recorded by Bruker axS D8 diffractometer with nickel filtered Cu-K $\alpha$  ( $\lambda = 1.5418 \text{ \AA}$ ) where the x-ray tube was operated at 40KV and 30 mA, the spectra were scanned at 0.02 step size. The reaction product was analyzed by a Perkin-Elmer 8500 GC with FID detector.

### 3. Results and discussion

Figure 1 shows the XRD patterns of LUS-1 samples before and after the loading of NH<sub>4</sub>VO<sub>3</sub> complexes.

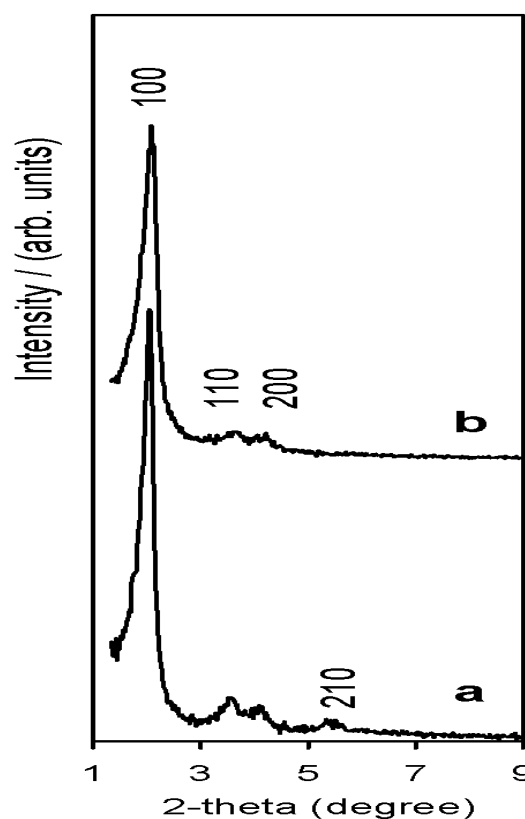
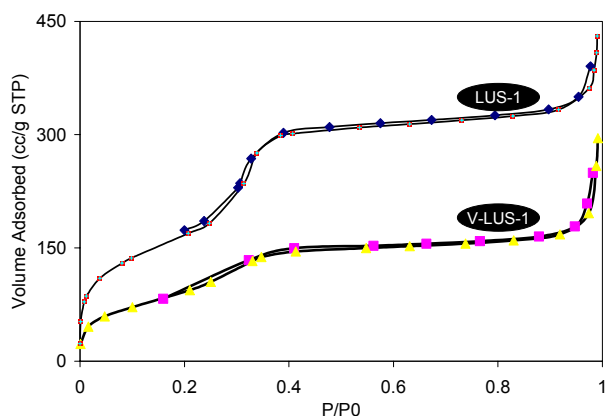


Fig.1. XRD patterns of (a) LUS-1 samples and (b) VO<sub>x</sub>/LUS-1.

As expected, the  $\text{VO}_x$  containing LUS-1 samples will exhibit their characteristic peaks assignable to hexagonal P6mm symmetry for LUS-1 sample. The spectra display the hexagonal symmetry with (100), (110), and (200) diffraction peaks. The XRD diffraction intensity is slightly reduced after the loading of  $\text{NH}_4\text{VO}_3$  complexes in the solid supports. The XRD patterns show that the loading of  $\text{NH}_4\text{VO}_3$  complexes in LUS-1 in solution do not affect the integrity of the well-defined mesostructure of solid supports. The decrease of intensity may arise from the larger contrast in the density from empty pores silica walls (LUS-1) and compare with the interred vanadium species into the pores ( $\text{VO}_x/\text{LUS-1}$ ).



**Fig. 2.** Nitrogen adsorption-desorption isotherms of LUS-1 and  $\text{VO}_x/\text{LUS-1}$ .

The nitrogen adsorption-desorption isotherms for LUS-1 and  $\text{VO}_x/\text{LUS-1}$  are shown in Figure 2. Both materials show type-IV adsorption behavior with the hysteresis loops appearing at relatively high pressure, suggesting that the prepared samples have regular mesoporous framework structures. Their texture properties are given in Table 1. The

surface area, average pore diameter calculated by the BET method and pore volume of  $\text{VO}_x/\text{LUS-1}$  are  $440 \text{ m}^2\text{g}^{-1}$ ,  $4.21 \text{ nm}$  and  $0.4267 \text{ cm}^3\text{g}^{-1}$ , respectively, which are smaller than those of LUS-1 due to the deposition of vanadium oxide into the pores.

**Table 1.** Surface area, pore size, and pore volume of  $\text{NH}_4\text{VO}_3$  complexes incorporated in the uncalcined samples of LUS-1 before and after the loading

Name	mmol of V/100g of sample	Surface Area ( $\text{m}^2/\text{g}$ )	Pore volume ( $\text{cm}^3/\text{g}$ )	Average pore diameter (nm)
LUS-1	-	620	0.67	4.3
$\text{VO}_x/\text{LUS-1}$	51	440	0.43	4.2

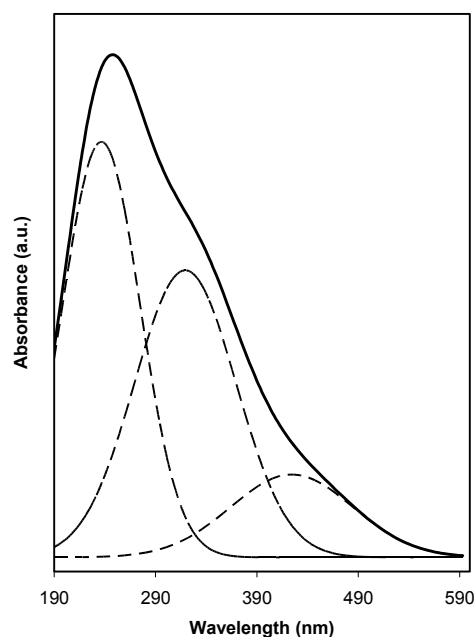
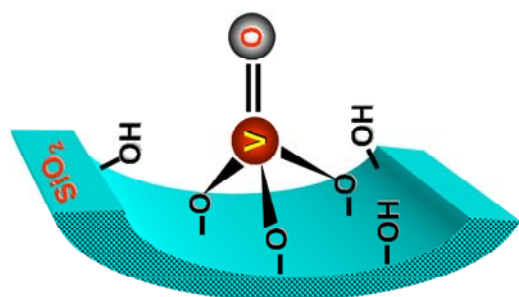


**Fig. 3.** UV-vis spectra of  $\text{VO}_x/\text{LUS-1}$ .

The nature of vanadium species on the  $\text{VO}_x/\text{LUS-1}$  was studied by UV-vis spectroscopy (Fig. 3). It generally provides valuable information about the coordination environments and oxidation states of vanadium [19-20]. The UV-vis shows

three bands at ca. 240, 315, 430 nm. The band at 240 and 315 nm can be attributed to charge transfer (CT) between  $O^{2-}$  and a center  $V^{5+}$  ion, as already observed for centers in zeolitic structures [21]. The CT band at higher energy (lower wavelength) can be ascribed to isolated monomeric tetrahedral vanadium species (scheme 1).



Scheme 1:

The presence of one-dimensional oligomeric units connected by V-O-V bands up to distorted tetrahedral coordination can be observed at the strong band at 315 nm. The third band at lower energy (430 nm) can be ascribed to distorted octahedral  $V^{5+}$  species. Similar UV-vis spectra have been previously reported for V-MCM-41, V-MCM-48, V-HMS, and V-SiO<sub>2</sub> [22-25]. Furthermore, the semi-quantitative calculations of the peak fitting values shows that vanadium species in VO<sub>x</sub>/LUS-1 exist mostly in tetrahedral VO<sub>x</sub> and much less in octahedral.

The texture results and UV-vis indicated that vanadium species are easily accessible to organic molecules. Thus, VO<sub>x</sub>/LUS-1 with high oxidation state of vanadium can be a good candidate for redox catalytic reaction.

### 3.1 Catalytic Activities

Base on the literature, all reactions were accomplished at 60 °C (temperature above 80 °C causes decomposition of H<sub>2</sub>O<sub>2</sub>) [26]. Table 2 presents the results of the influence of the various solvents (such as acetic acid, methanol, acetone, and acetonitrile) on the catalytic hydroxylation of benzene using H<sub>2</sub>O<sub>2</sub> as oxidant by VO<sub>x</sub>-LUS-1.

**Table 2.** Effect of the solvent direct oxidation of benzene to phenol in liquid phase by H<sub>2</sub>O<sub>2</sub> over VO<sub>x</sub>/LUS-1.

Solvent	PHE <sup>a</sup> (%)	BEN <sup>b</sup> (%)	HYD <sup>c</sup> (%)	BIP <sup>d</sup> (%)	Ben <sup>e</sup> CONV (%)	SEL <sup>f</sup> (%)
acetic acid	25.0	4.4	2.0	2.0	34.0	73.5
methanol	16.0	1.3	2.4	3.8	24.0	66.7
acetone	2.2	0.2	1.1	1.0	4.5	48.9
acetonitry	1.7	0.4	0.2	0.3	2.8	60.1

<sup>a</sup>:phenol;

<sup>b</sup>: 1,4-benzoquinone;

<sup>c</sup>:1,4-hydroquinone;

<sup>d</sup>:biphenyl;

<sup>e</sup>:benzene conversion = mmol product/mmol initial benzene;

<sup>f</sup>:selectivity= mmol phenol /mmol product.

It is noteworthy here that the reaction yield and selectivity were strongly affected by the nature of the solvent. The maximum yield and selectivity of the phenol produced was obtained in the presence of acetic acid. It can be attributed to the stabilization of H<sub>2</sub>O<sub>2</sub> as peroxy acetic acid species in the radical mechanism and the formation of a vanadoperoxide complex. It has been proposed that the hydroxylation of the aromatic ring over modified metal oxides by H<sub>2</sub>O<sub>2</sub> occurs via the heterolytic mechanism, involving the formation of a metalloperoxide species, while

oxyfunctionalization of a side chain proceeds through the radical pathway [27–29]. Thus, we can suggest that acetic acid interaction by hydrogen peroxide over VO<sub>x</sub>/LUS-1 and produced acetoxy radicals. These radicals may be coordinated with vanadium in VO<sub>x</sub>/LUS-1 to form a peroxy group on vanadium ion (active center) (Fig. 4). Then, this active center attacked of the adsorbed benzene and output benzyl radicals in the next section reaction by hydroxyl radicals genesis of decomposition of hydrogen peroxide over vanadium segment and produced phenol [30, 31].

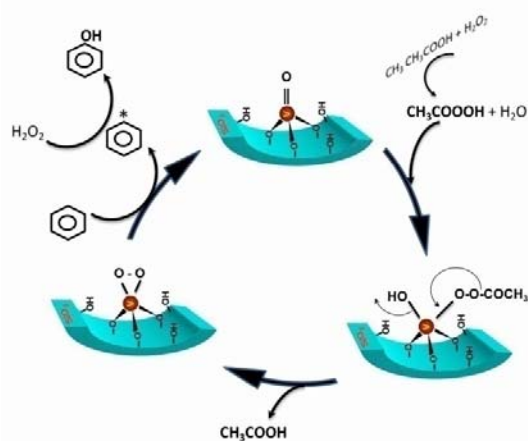


**Fig. 4.** Scheme of hydroxylation of benzene by H<sub>2</sub>O<sub>2</sub> VO<sub>x</sub>/LUS-1 in acetic acid.

Finally, the catalytic performance of the recovered catalyst was also checked. The catalyst was recovered by filtration, regenerated by soxhlet extraction using acetone, dried at 100 °C under vacuum for 3 h and reused several times. It was found that the vanadium leached about 1.5 % which may be due to leaching of the remaining vanadium ions on the surface. Leaching was markedly decreased after the first reuse and almost stopped after the second cycle. The yield of phenol

was lowered by 2–4% but reserved its selectivity after four times reused of catalyst.

#### 4. Conclusion

In conclusion, vanadium supported on highly ordered nanoporous silica (VO<sub>x</sub>-LUS-1) was synthesized and characterized of showed ordered structural patterns for the catalyst prepared. Direct oxidation of benzene to phenol in liquid phase by H<sub>2</sub>O<sub>2</sub> peroxide were examined over this catalyst by using various (methanol, acetone, acetic acid, acetonitril) solvents. The maximum yield and selectivity of the phenol produced was obtained in the presence of acetic acid. It was proposed that the oxidation of benzene to phenol by peroxy acetic acid (CH<sub>3</sub>OOH + H<sub>2</sub>O<sub>2</sub> → CH<sub>3</sub>COOOH) occur via heterolytic mechanism, involving the formation of a vanadoperoxide complex. The catalyst can be reused for several times without any appreciable loss of activity.

#### References

- [1] D. Bianchi, I. Balducci, R. Botelo, R. Daloisio, M. Rieci, G. Spano, R. Tassinari, C. Toniniand, R. Ungarelli, *Adv. Synth. Catal.* 349 (2007) 979.
- [2] K. Weissermehl, H. J. Arpe: *Industrielle Organische Chemie*, VCH, Weinheim, 1998.
- [3] S. Niwa, M. Eswaramoorthy, J. Nair, A. Raj, N. Itoh, H. Shoji, T. Namba F. Mizukami, *Science*, 295 (2002) 105.
- [4] D. Bianchi, R. Bortolo, R. Tassinari, M. Ricci, R. Vignola, *Angew. Chem. Int. Ed.*, 39 (2000) 4321.

- [5] L. Balducci, D. Bianchi, R. Bortolo, R. D'Aloisio, M. Ricci, R. Tassinari, R. Ungarelli, *Angew. Chem. Int. Ed.*, 42 (2003) 4937
- [6] M. Tani, T. Sakamoto, S. Mita, S. Sakaguchi, Y. Ishii, *Angew. Chem. Int. Ed.*, 117 (2005) 2642.
- [7] A. Bhaumik, P. Mukherjee, R. Kumar<sup>1</sup>, *J. Catal.* 178 (1998) 101.
- [8] A. Corma, V. Fornés, S. Iborra, M. Mifsud, M. Renz, *J. Catal.* 221 (2004) 67.
- [9] W. T. Dixon, R. O. C. Norman, *J. Chem. Soc.* 4 (1976) 4857.
- [10] K. Lemke, K. Jähnisch, H. Ehrich, U. Lohse, H. Berndt, *Appl. Catal.* 243 (2003) 41.
- [11] S. Yamaguchi, S. Sumimoto, Y. Ichihashi, S. Nishiyama, Shigeru Tsuruya, *Ind. Eng. Chem. Res.* 44 (2005) 1.
- [12] Y. Tang, J. Zhang, *Tran. Metal. Chem.* 31(2006) 299.
- [13] J. Zhang, Y. Tang, G. Li, C. Hu, *Appl. Catal. A, Gen.* 278( 2005) 251.
- [14] Y. Masumoto, R. Hamada, K. Yokota, S. Nishiyama, Shig, *Appl. Catal. A*.184 (2005) 215.
- [15] Y. W. Chen and Y. H. Lu, *Ind. Eng. Chem. Res.* 38 (1999) 1893.
- [16] Y. Gu, X. Zhao, G. Zhang, H. Diong, Y. Shan, *Appl. Catal. A*. 328 (2007) 150.
- [17] L. Bonnevot, M. Morin, A. Badiei, Patent WO 01/55031 A1, 2001.
- [18] A. Badiei, L. Bonnevot, N. Crowther, G. Mohammadi Ziarani, *J. Organomet. Chem.* 691 (2006) 5911.
- [19] P. Van der Voort, M. Morey, G.D. Stucky, M. Mathieu, E.F. Vansant, *J. Phys. Chem. B* 102 (1998) 585.
- [20] M. Morey, A. Davidson, H. Eckert, G. Stucky, *Chem. Mater.* 8 (1996) 482.
- [21] Z. Luan, J. Xu, H. He, J. Klinowski, L. Kevan: *J. Phys. Chem.*, 100 (1996) 19595.
- [22] L. Chia-Hung, L. Tien-Sung, M. Chung-Yuan, *J. Phys. Chem.* 111 (2007) 3873.
- [23] S. Shylesh, S.P. Mirajkar, A.P. Singh, *J. Mol. Catal. A: Chem.* 239 (2005) 57.
- [24] A. Tuel, *Micropor Mesopor. Mater.* 27 (1999) 151.
- [25] K. Geon-Joong, C. Dong-Su, K. Kwang-Ho, K. Wan-Suk, K. Jong-Ho, S. Hiroshi, *Catal. Lett.* 31 (1995) 91.
- [26] T. Radhika, S. Sugunan, *J. Mol. Catal. A: Chem.* 250 (2006) 169.
- [27] R. Neumann, M. Levin-Elad, *Appl. Catal. A* 122 (1995) 85.
- [28] D. R. C. Huybrechts, P. L. Buskens, P. A. Jacobs, *J. Mol. Catal.* 71 (1992) 129.
- [29] K. Bahranowski, R. Dula, M. Gasior, M. Labanowska, A. Michalik, L. A. Vartikian, E. M. Serwicka, *Appl. Clay Sci.* 18 (2001) 93.
- [30] M. Iwamoto, J. Hirata, K. Matsukami, S. Kagawa, *J. Phys. Chem.* 87 (1983) 903.
- [31] S. E. Dapurkar, A. Sakthivel, P. Selvam, *J. Mol. Catal. A: Gen.* 223 (2004) 241.